Hindawi Publishing Corporation
Journal of Nanomaterials
Volume 2012, Article ID 317857, 5 pages
doi:10.1155/2012/317857

Research Article

Sonochemical Synthesis of Er^{3+}-Doped ZnO Nanospheres with Enhanced Upconversion Photoluminescence

Jun Geng,[1,2] Guang-Hui Song,[1] and Jun-Jie Zhu[1]

[1] *State Key Laboratory of Analytical Chemistry for Life Science, School of Chemistry and Chemical Engineering, Nanjing University, Nanjing 210093, China*
[2] *Department of Chemistry, Jiangsu Institute of Education, Nanjing 210013, China*

Correspondence should be addressed to Jun-Jie Zhu, jjzhu@nju.edu.cn

Received 24 September 2012; Accepted 8 October 2012

Academic Editor: Xiao-Miao Feng

Er^{3+}-doped ZnO nanospheres have been synthesized via a sonochemical conversion process. The formation mechanism of these nanocrystals is connected with the sonochemical effect of ultrasound irradiation. The as-prepared Er^{3+} doped ZnO nanospheres show enhanced photoluminescence and upconversion photoluminescence properties compared with pure ZnO.

1. Introduction

ZnO semiconductors, with a direct wide bandgap of 3.37 eV and aesthetic nanoscale morphologies, have been intensively studied due to their multifunctional characteristics for a diverse range of applications in optical, electronic, optoelectronic, piezoelectric, photocatalytic, and power devices [1]. In the past decade, ZnO has been explored for new device applications when extra functionalities are intentionally introduced through proper doping or alloying with impurity ions despite the considerable challenges. It is worth noting that much effort has also been made through doping rare earth (RE) ions (e.g., Er^{3+} and Eu^{3+}) into the ZnO host, which undergoes upconversion (UC) luminescence and/or energy transfer, in realizing new optoelectronic and photonic device applications such as solid-state full-colour displays, infrared detectors, solar cells, biological fluorescent labels, and all-solid compact lasers [2]. The Er^{3+}-doped semiconductors are the potential optoelectronic materials [3] due to the Er intra-4f shell transition with a photoemission at a wavelength of 1.54 μm, which lies in the minimum loss region of silica-based optical fibers [4].

Up to now, physical doping methods such as ion implantation [5], laser ablation [6], magnetron sputtering [7], and high temperature calcinations [8] have mainly been used to introduce Er into ZnO substrate, while most researches focused on the formation of films. Some chemical doping methods, such as sol-gel [9], colloidal [10], and hydrothermal processes [11], have also been reported to prepare Er^{3+}-doped ZnO nanocrystals. However, most products were nanoparticles. Only a few groups reported the morphology-controlled synthesis, such as Er^{3+}-doped ZnO nanowires fabricated using Er-ion implantation [5], flower-like structures prepared by a wet chemical reaction [12], and prickly sphere-like, column-like, prism-like, and grain-like structures prepared via hydrothermal process [13]. Therefore, it is still a challenge to prepare Er^{3+}-doped nanocrystals with special morphology through a fast and convenient method.

Here, a facile sonochemical route has been used to prepare Er^{3+}-doped ZnO nanospheres. Under the irradiation of ultrasound, it only took 30 min of reaction time to effectively dope Er^{3+} into ZnO host. The photoluminescence and upconversion photoluminescence properties of the as-prepared Er^{3+}-doped ZnO nanospheres were investigated, and the results showed enhanced emission due to effective doping.

2. Experimental

2.1. Materials. All the reagents used were of analytical purity and were used without further purification.

$Zn(NO_3)_2 \cdot 6H_2O$, $Er(NO_3)_3 \cdot 5H_2O$, PEG-20000, and triethanolamine (TEA) were purchased from Beijing Chemical Reagents Ltd. Co. of China.

2.2. Synthesis. Typically, $Zn(NO_3)_2 \cdot 6H_2O$ (0.005 mol) was dissolved in H_2O (100 mL), and then specific amount of $Er(NO_3)_3 \cdot 5H_2O$ (2, 5, 10% doping, resp.), PEG-20000 (1 g) and TEA (2 mL) were introduced sequentially with stirring to form a clear solution. The transparent mixture solution was exposed to high-intensity ultrasound irradiation under ambient air for 30 min. Ultrasound irradiation was generated with a high-intensity ultrasonic probe (Xinzhi Co., China, JY92-2D, 0.6 cm diameter; Ti-horn, 20 kHz, 60 W cm^{-2}) immersed directly in the reaction solution. A white precipitate was centrifuged, washed with distilled water and absolute ethanol in sequence, and finally dried in air. The final products were collected for characterizations and further preparations.

2.3. Characterization. The X-ray powder diffraction (XRD) analysis was performed on a Philips X'-pert X-ray diffractometer at a scanning rate of 4° min^{-1} in the 2θ range from 10° to 80°, with graphite-monochromatized Cu-$K\alpha$ radiation (λ = 0.15418 nm). The scanning electron micrographs (SEM) were taken on a LEO-1530VP field-emission scanning electron microscope. Transmission electron microscopy (TEM) was carried out on a JEOLJEM 200CX transmission electron microscope, using an accelerating voltage of 200 kV. High-resolution transmission electron micrographs (HRTEM) were obtained by employing a JEOL-2010 high-resolution transmission electron microscope with an accelerating voltage of 200 kV. Photoluminescence spectra (PL) were measured on a Shimadzu RF-5301PC fluorescence spectrometer under the excitation of 325 nm at room temperature. The upconversion (UC) photoluminescence spectra were recorded on a spectrometer (Zolix, China) equipped with a 980 nm laser diode as the excitation source.

3. Results and Discussion

3.1. Characterization of the Final Products. Figure 1 shows the XRD pattern of the as-prepared products. Evidently, all of the diffraction peaks in the XRD pattern are well assigned to hexagonal wurtzite ZnO as reported in JCPDS card no. 36-1451, and no impurity phase related to Er^{3+} could be found. The diffraction peaks shift to lower angel slightly with the Er-doping concentration increasing from 2–10%, indicating that the lattice parameter gets larger when Er^{3+} are incorporated into ZnO lattice, which is consistent with the fact that the radii of Er^{3+} (R = 0.89 Å) are bigger than that of Zn^{2+} (R = 0.74 Å).

The as-prepared Er^{3+}-doped ZnO samples appeared as uniform solid nanospheres with diameter of ca. 400 nm, as shown in Figures 2(a) and 2(b). The HRTEM image recorded on the surface of ZnO : Er nanospheres (Figure 2(c)) shows lattice fringes with interplanar spacing of 0.25 nm for the (101) faces of hexagonal ZnO.

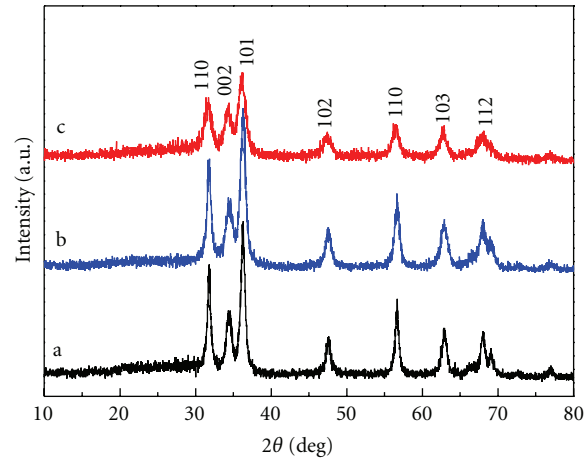

FIGURE 1: XRD patterns of Er^{3+}-doped ZnO nanocrystals with Er doping concentrations of (a) 2%, (b) 5%, and (c) 10%.

3.2. Possible Sonochemical Formation Mechanism. In recent years, ultrasonic irradiation has been extensively used in the synthesis of nanomaterials. The effects of high-intensity ultrasound result primarily from acoustic cavitation are [14]: the formation, growth, and implosive collapse of bubbles in liquids. During the acoustic cavitation process, very high temperatures (>5000 K), pressures (>20 MPa), and cooling rates (>10^{10} K s^{-1}) can be achieved upon the collapse of the bubble, which provides a unique platform for the growth of nanostructures including 0D nanoparticles [15], 1D nanorods [16], to 2D nanoplates [17], and even mesoporous [18] or hollow structures [19]. Nanocomposites [20] and doped nanomaterials [21] have also been prepared through sonochemical methods.

In the present case, $Zn(NO_3)_2 \cdot 6H_2O$ was used as precursor, TEA as complexing and precipitating agent and PEG as capping agent. TEA has the chemical formula $N(CH_2CH_2OH)_3$, which acts generally as a weak base due to the single lone pair of electrons on nitrogen atom and accordingly could coordinate to zinc ions forming $[Zn(TEA)_4]^{2+}$ complex [22]. Under ultrasonic irradiation, the complex would dissociate and a part of TEA molecules would hydrolyze to build up an alkaline environment, which leads to the controlled release of free zinc ions and hydroxide ions ((1) and (2)). The released Zn^{2+} ion and OH^- ion would combine and transform to ZnO under sonochemical conditions ((3) and (4)). As a popular shape modifier, PEG was used here to control the morphology of formed ZnO nanoparticles and also showed effective role to make uniform ZnO nanospheres. Therefore, the mechanism of the formation of ZnO nanospheres is probably related to the coordination of Zn^{2+} and TEA to form Zn-TEA complex, the dissociation of the complex under sonication and PEG-modified formation of ZnO nanospheres. The probable reaction process in aqueous solution can be summarized as follows:

$$[Zn(TEA)_4]^{2+} \text{ complex} \longrightarrow Zn^{2+} + 4TEA, \quad (1)$$

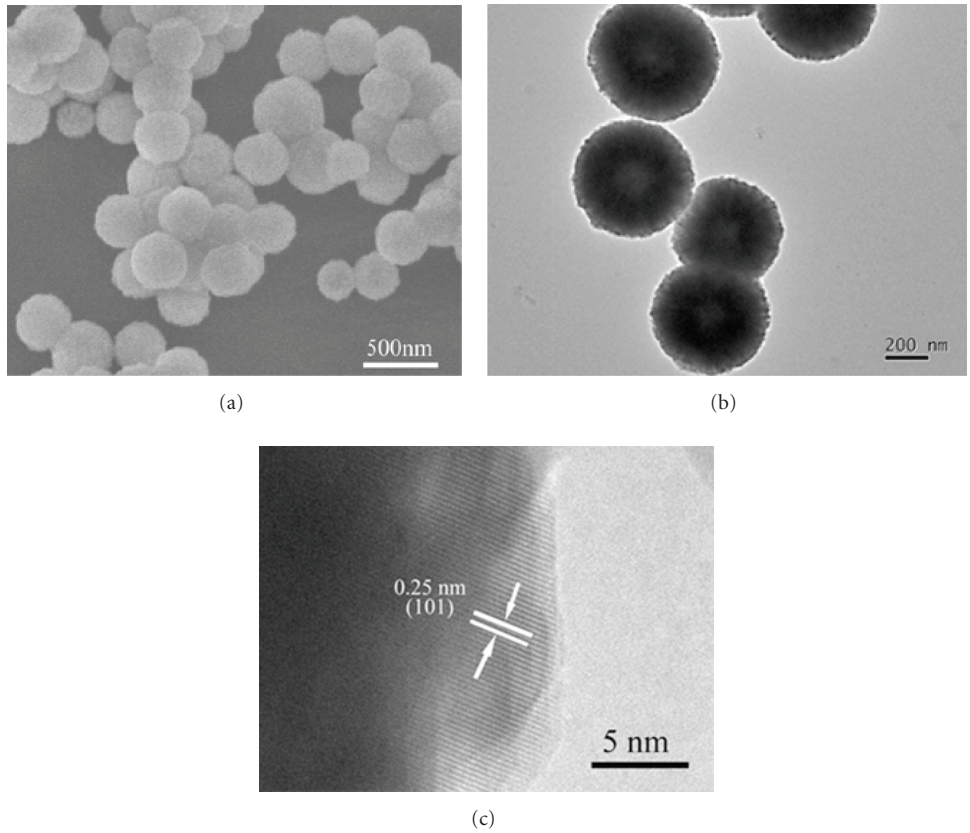

(a) (b)

(c)

Figure 2: (a) SEM, (b) TEM, and (c) HRTEM images of the as-prepared Er^{3+}-doped ZnO nanospheres with Er doping concentration of 2%.

$$\mathrm{TEA} + \mathrm{H_2O} \longleftrightarrow [\mathrm{TEA}]^{+} + \mathrm{OH}^{-}, \quad (2)$$

$$\mathrm{Zn}^{2+} + 2\mathrm{OH}^{-} \longrightarrow \mathrm{Zn(OH)_2}, \quad (3)$$

$$\mathrm{Zn(OH)_2} \longrightarrow \mathrm{ZnO} + \mathrm{H_2O}. \quad (4)$$

High-intensity ultrasonic irradiation also played an important role. The transient high temperature and high pressure field produced during ultrasonic irradiation provides a favorable environment for the growth of nanocrystals. Cavitations and shock waves created by ultrasound can accelerate solid particles to high velocities leading to interparticle collisions and inducing effective fusion at the point of collision [23]. We consider that the high temperature, high pressure, and shock waves caused by ultrasound induced the effective doping of Er^{3+} into ZnO host. The energy generated during collision can induce the crystallization of the amorphous particles, responsible for the further crystallization process. It only took 30 min of reaction time to conduct effective doping under ultrasonic irradiation, while rather long reaction time (e.g., 8–12 hours) is needed in hydrothermal and other synthetic routes.

3.3. Photoluminescence Properties. Figure 3 shows the room-temperature photoluminescence spectra of pure and Er^{3+}-doped ZnO with different Er^{3+} doping concentrations using the same excitation line at 325 nm. All samples show a strong and broad green emission around 540 nm which can be attributed to deep-level emission (DLE) caused by defects and impurities [24]. The emission intensity of ZnO : Er is increased enormously as compared with that of undoped ZnO. The integral emission intensity of ZnO : Er with 10% Er^{3+} doping concentration is 3 times higher than that of the undoped ZnO, which indicates an unusual improvement on the light yield by Er doping.

The PL spectra of the ZnO : Er crystal with Er^{3+} doping concentration varying from 2% to 10% (Figures 3(b)–3(d)) show that the emission intensity enhanced with the increasing doping concentration. The heavily doped product appeared to have an extremely high PL intensity in the present case, which might be related to the interaction between ZnO and Er. Previous studies reported that the intentionally doped impurities could provide a significant contribution to DLE, for example, by providing donor-acceptor pairs in ZnO [24]. The majority of Er in ZnO is likely to be associated with rare earths occupying substitutional Zn sites [25], and the local lattice is modified because of the different oxidation states and ionic sizes of Er and Zn ions [26]. The incorporation of Er ions in the ZnO lattice is therefore expected to increase the deep-level states and resulted in an increase in DLE. Energy transfer might also occur between excitons and Er^{3+} ions [27]; however, we did not observe Er^{3+} emission peaks in the visible region. It might be possible that the weak emission peaks of Er^{3+} ions were embedded in the trace of a strong DLE.

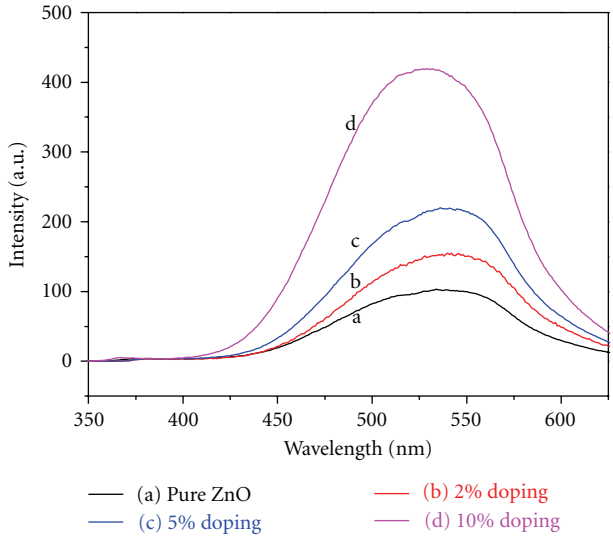

Figure 3: The PL spectra of (a) the pure ZnO and Er^{3+}-doped ZnO nanospheres with different Er doping concentrations of (b) 2%, (c) 5%, and (d) 10%.

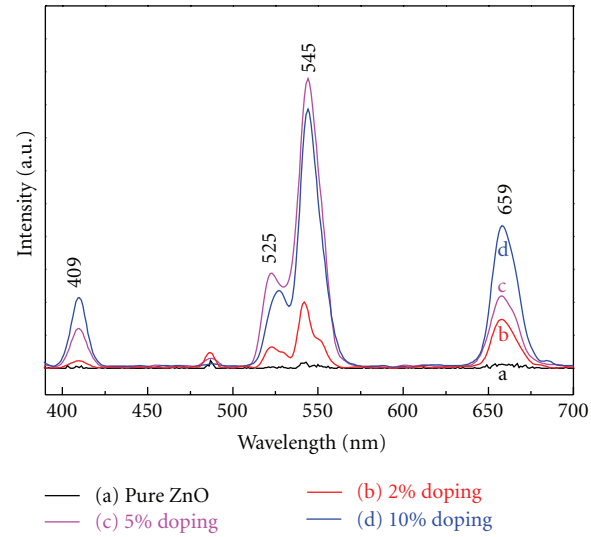

Figure 4: Upconversion spectra of (a) the pure ZnO and Er^{3+}-doped ZnO nanospheres with different doping concentrations of (b) 2%, (c) 5%, and (d) 10% excited by 980 nm laser at room temperature.

3.4. Upconversion Luminescence Properties. Upon excitation with a 980 nm semiconductor laser diodes (SLD) at room temperature, the blue, green, and red upconversion emissions of Er^{3+} ions in the ZnO nanocrystals were observed, which suggests that the Er^{3+} ions have been incorporated inside the crystalline ZnO grains. The upconversion luminescence spectra for the pure ZnO and Er^{3+}-doped ZnO nanospheres with different Er doping concentrations are shown in Figure 4, where four emission bands at approximately 409 nm, 525, 545, and 659 nm are assigned to $2H_{9/2}$ to $4I_{15/2}$, $2H_{11/2}$ to $4I_{15/2}$, $4S_{3/2}$ to $4I_{15/2}$, and $4F_{9/2}$ to $4I_{15/2}$ transitions, respectively [2].

Obviously, the upconversion luminescence intensity of Er^{3+}-doped ZnO is much higher than that of pure ZnO, which indicate the effective doping could enhance the upconversion emission. It is found that with the Er doping concentration increasing from 2% to 5%, the integral upconversion luminescence intensity enhanced. However, with the Er-doping concentration varying from 5% to 10%, the green emission decreased slightly while the red emission enhanced, which is similar with the literature [28]. Therefore, the upconversion light output could be tuned by adjusting the dopant concentration. Further detailed investigation is still going on.

4. Conclusion

Er^{3+}-doped ZnO nanospheres have been synthesized via a facile sonochemical route. Ultrasonic irradiation played an important role in the formation of ZnO nanospheres and resulted in the effective doping. The photoluminescence intensity of Er^{3+}-doped nanocrystals enhanced with the increasing Er doping concentrations. Higher upconversion photoluminescence emissions of the Er^{3+}-doped ZnO nanocrystals were observed, which suggests that the Er^{3+} ions have been incorporated inside the crystalline ZnO grains.

Acknowledgments

This work is supported by the Young Scientists Fund of the National Natural Science Foundation of China (Grant no. 20805022), National Natural Science Foundation of China (Grant no. 50972058), and China Postdoctoral Science Foundation (Grant no. 20100471294).

References

[1] Z. L. Wang and J. Song, "Piezoelectric nanogenerators based on zinc oxide nanowire arrays," *Science*, vol. 312, no. 5771, pp. 243–246, 2006.

[2] X. Wang, X. Kong, G. Shan et al., "Luminescence spectroscopy and visible upconversion properties of Er^{3+} in ZnO nanocrystals," *Journal of Physical Chemistry B*, vol. 108, no. 48, pp. 18408–18413, 2004.

[3] Y. Bai, Y. Wang, K. Yang et al., "The effect of Li on the spectrum of Er^{3+} in Li- and Er-codoped ZnO nanocrystals," *Journal of Physical Chemistry C*, vol. 112, no. 32, pp. 12259–12263, 2008.

[4] X. Zhao, S. Komuro, H. Isshiki, Y. Aoyagi, and T. Sugano, "Fabrication and stimulated emission of Er-doped nanocrystalline Si waveguides formed on Si substrates by laser ablation," *Applied Physics Letters*, vol. 74, no. 1, pp. 120–122, 1999.

[5] K. Zhong, J. Xu, J. Su, and Y. L. Chen, "Upconversion luminescence from Er-N codoped of ZnO nanowires prepared by ion implantation method," *Applied Surface Science*, vol. 257, no. 8, pp. 3495–3498, 2011.

[6] S. Harako, S. Yokoyama, K. Ide, X. Zhao, and S. Komoro, "Visible and infrared electroluminescence from an Er-doped n-ZnO/p-Si light emitting diode," *Physica Status Solidi A*, vol. 205, no. 1, pp. 19–22, 2008.

[7] Y. Chen, X. L. Xu, G. H. Zhang, H. Xue, and S. Y. Ma, "Blue shift of optical band gap in Er-doped ZnO thin films deposited by direct current reactive magnetron sputtering technique," *Physica E*, vol. 42, no. 5, pp. 1713–1716, 2010.

[8] Z. Zhou, T. Komori, T. Ayukawa et al., "Li- and Er-codoped ZnO with enhanced 1.54 μm photoemission," *Applied Physics Letters*, vol. 87, no. 9, Article ID 091109, 3 pages, 2005.

[9] X. Meng, C. Liu, F. Wu, and J. Li, "Strong up-conversion emissions in ZnO:Er^{3+}, ZnO:Er^{3+}-Yb^{3+} nanoparticles and their surface modified counterparts," *Journal of Colloid and Interface Science*, vol. 358, no. 2, pp. 334–337, 2011.

[10] M. Kohls, T. Schmidt, H. Katschorek et al., "Simple colloidal route to planar micropatterned ErZnO amplifiers," *Advanced Materials*, vol. 11, no. 4, pp. 288–292, 1999.

[11] C.-Y. Chen, K.-Y. Lai, J.-W. Lo et al., "Electronic structures of well-aligned Er-doped ZnO nanorod arrays," *Journal of Nanoscience and Nanotechnology*, vol. 11, no. 12, pp. 10615–10619, 2011.

[12] W. C. Yang, C. W. Wang, J. H. He et al., "Facile synthesis of large scale Er-doped ZnO flower-like structures with enhanced 1.54 μm infrared emission," *Physica Status Solidi A*, vol. 205, no. 5, pp. 1190–1195, 2008.

[13] Y. Sun, Y. Chen, L. Tian et al., "Morphology-dependent upconversion luminescence of ZnO:Er^{3+} nanocrystals," *Journal of Luminescence*, vol. 128, no. 1, pp. 15–21, 2008.

[14] K. S. Suslick, S. B. Choe, A. A. Cichowlas, and M. W. Grinstaff, "Sonochemical synthesis of amorphous iron," *Nature*, vol. 353, no. 6343, pp. 414–416, 1991.

[15] A. Nemamcha, J. L. Rehspringer, and D. Khatmi, "Synthesis of palladium nanoparticles by sonochemical reduction of palladium(II) nitrate in aqueous solution," *Journal of Physical Chemistry B*, vol. 110, no. 1, pp. 383–387, 2006.

[16] J. Geng, W. H. Hou, Y. N. Lv, J. J. Zhu, and H. Y. Chen, "One-dimensional BiPO4 nanorods and two-dimensional BiOCl lamellae: fast low-temperature sonochemical synthesis, characterization, and growth mechanism," *Inorganic Chemistry*, vol. 44, no. 23, pp. 8503–8509, 2005.

[17] L. P. Jiang, S. Xu, J. M. Zhu, J. R. Zhang, J. J. Zhu, and H. Y. Chen, "Ultrasonic-assisted synthesis of monodisperse single-crystalline silver nanoplates and gold nanorings," *Inorganic Chemistry*, vol. 43, no. 19, pp. 5877–5883, 2004.

[18] R. K. Rana, Y. Mastai, and A. Gedanken, "Acoustic cavitation leading to the morphosynthesis of mesoporous silica vesicles," *Advanced Materials*, vol. 14, no. 19, pp. 1414–1418, 2002.

[19] J. Geng, J. J. Zhu, D. J. Lu, and H. Y. Chen, "Hollow PbWO4 nanospindles via a facile sonochemical route," *Inorganic Chemistry*, vol. 45, no. 20, pp. 8403–8407, 2006.

[20] J. Geng, X. D. Jia, and J. J. Zhu, "Sonochemical selective synthesis of ZnO/CdS core/shell nanostructures and their optical properties," *CrystEngComm*, vol. 13, no. 1, pp. 193–198, 2011.

[21] J. Geng, D. Lu, J. J. Zhu, and H. Y. Chen, "Antimony(III)-doped $PbWO_4$ crystals with enhanced photoluminescence via a shape-controlled sonochemical route," *Journal of Physical Chemistry B*, vol. 110, no. 28, pp. 13777–13785, 2006.

[22] Y. S. Fu, X. W. Du, J. Sun, Y. F. Song, and J. Liu, "Kinetics controlled growth of quasi-spherical ZnO single crystal in homogeneous solutions," *Journal of Alloys and Compounds*, vol. 461, no. 1-2, pp. 527–531, 2008.

[23] S. J. Doktycz and K. S. Suslick, "Interparticle collisions driven by ultrasound," *Science*, vol. 247, no. 4946, pp. 1067–1069, 1990.

[24] N. Y. Garces, L. Wang, L. Bai, N. C. Giles, L. E. Halliburton, and G. Cantwell, "Role of copper in the green luminescence from ZnO crystals," *Applied Physics Letters*, vol. 81, no. 4, pp. 622–624, 2002.

[25] U. Wahl, E. Rita, J. G. Correia, E. Alves, and J. P. Araújo, "Implantation site of rare earths in single-crystalline ZnO," *Applied Physics Letters*, vol. 82, no. 8, pp. 1173–1175, 2003.

[26] Z. Zhou, T. Komori, M. Yoshino et al., "Enhanced 1.54 μm photoluminescence from Er-containing ZnO through nitrogen doping," *Applied Physics Letters*, vol. 86, no. 4, Article ID 041107, 3 pages, 2005.

[27] S. Komuro, T. Katsumata, T. Morikawa, X. Zhao, H. Isshiki, and Y. Aoyagi, "Highly erbium-doped zinc-oxide thin film prepared by laser ablation and its 1.54 μm emission dynamics," *Journal of Applied Physics*, vol. 88, no. 12, pp. 7129–7136, 2000.

[28] Y. Liu, C. Xu, and Q. Yang, "White upconversion of rare-earth doped ZnO nanocrystals and its dependence on size of crystal particles and content of Yb^{3+} and Tm^{3+}," *Journal of Applied Physics*, vol. 105, no. 8, Article ID 084701, 6 pages, 2009.